

UC Irvine

UC Irvine Previously Published Works

Title

Electron spin resonance of the intermetallic antiferromagnet EuIn_2As_2

Permalink

<https://escholarship.org/uc/item/18v6s6sm>

Journal

Physical Review B, 86(9)

ISSN

2469-9950

Authors

Rosa, PFS
Adriano, C
Garitezi, TM
[et al.](#)

Publication Date

2012-09-01

DOI

10.1103/physrevb.86.094408

Copyright Information

This work is made available under the terms of a Creative Commons Attribution License, available at <https://creativecommons.org/licenses/by/4.0/>

Peer reviewed

Electron spin resonance of the intermetallic antiferromagnet EuIn_2As_2 P. F. S. Rosa,^{1,3} C. Adriano,^{1,3} T. M. Garitezi,¹ R. A. Ribeiro,² Z. Fisk,³ and P. G. Pagliuso^{1,3}¹*Instituto de Física “Gleb Wataghin”, Universidade Estadual de Campinas, Campinas SP 13083-859, Brazil*²*Centro de Ciências Naturais e Humanas, Universidade Federal do ABC, Santo André SP 09210-170, Brazil*³*University of California, Irvine, California 92697, USA*

(Received 4 July 2012; revised manuscript received 21 August 2012; published 7 September 2012)

We present electron spin resonance (ESR) measurements in single-crystalline samples of EuIn_2As_2 grown using the In-flux method. This compound crystallizes in a hexagonal $P6_3/mmc$ structure and presents antiferromagnetic (AFM) ordering below $T_N = 16$ K. In the paramagnetic state, a single Eu^{2+} Dysonian ESR line with nearly temperature-independent g -factor and linewidth is observed, indicating the absence of Korringa-like relaxation of the Eu^{2+} ions. Approaching the AFM transition, we observe an anisotropic g -shift and a linewidth broadening which has a maximum at T_N , suggesting that the short-range AFM correlation dominates the spin dynamics of the Eu^{2+} spins in this temperature range. Our results are discussed based on complementary data (magnetic susceptibility, heat capacity, and electrical resistivity measurements) that provide further details about the global macroscopic physical properties of the EuIn_2As_2 intermetallic compound.

DOI: [10.1103/PhysRevB.86.094408](https://doi.org/10.1103/PhysRevB.86.094408)

PACS number(s): 76.30.-v, 71.20.Lp

I. INTRODUCTION

Rare-earth based intermetallic series of compounds are usually of great interest to explore the interplay between Ruderman-Kittel-Kasuya-Yoshida (RKKY) magnetic interaction, crystalline electric-field (CEF) effects, and Fermi surface (FS) effects commonly present in these materials. For instance, the series of intermetallics RM_2T_2 (122 system, $M = \text{e.g., Fe, Cu, Ni, Rh, Ru}$; $T = \text{e.g., Si, Ge, As}$) were systematically studied due to their large variety of interesting physical properties such as heavy-fermion (HF) behavior, unconventional superconductivity (SC), and complex magnetic structures.^{1,2}

Recently, the discovery of superconducting doped iron arsenide oxides, RFeAsO (1111 system) with $R = \text{La-Gd}$, has triggered many efforts to synthesize new materials with FeAs layers that ultimately brought back to the scene the 122 family with the discovery of an oxygen-free new family of superconductors AFe_2As_2 with $A = \text{Ba, Sr, Ca, Eu}$. These systems crystallize in the tetragonal ThCr_2Si_2 -type crystal structure ($I4/mmm$) and exhibit a spin-density-wave (SDW) phase transition with $100 \text{ K} \lesssim T_{\text{SDW}} \lesssim 300 \text{ K}$ which can be suppressed by both doping and applied pressure until a superconducting ground state appears.³

These compounds are speculated to be prototypes that play host to new superconductors. However, the magnetic properties of non-superconducting As-based magnetic 122 compounds have not been extensively explored yet. The study of magnetic analogs which are structurally related to unconventional superconductors has been found to be useful to help understand details of the magnetic interactions in these materials that may play a role for the occurrence of SC.³

In this paper we report the physical properties investigation of the intermetallic antiferromagnetic (AFM) EuIn_2As_2 . This compound crystallizes in the hexagonal $P6_3/mmc$ space group ($a = 4.207 \text{ \AA}$ and $c = 17.889 \text{ \AA}$) which contains layers of Eu^{2+} cations separated by $[\text{In}_2\text{As}_2]^{2-}$ layers along the crystallographic c -axis. The field-dependent magnetic susceptibility shows an anisotropy with respect to crystallographic orientation below $T \sim 45 \text{ K}$ and an AFM ordering at $T_N = 16 \text{ K}$. The

anisotropic low- T data also indicate that there are both strong ferromagnetic intralayer and weaker AFM interlayer magnetic interactions between the Eu^{2+} ions. Transport measurements revealed negative colossal magnetoresistance which presumably evolves to some extent from the magnetic scattering of the conduction electrons (CEs) by the Eu^{2+} spins.⁵

To further explore the physical properties of EuIn_2As_2 and to elucidate the microscopic details of the Eu^{2+} ions magnetic interactions we have performed electron spin resonance (ESR) experiments in EuIn_2As_2 single crystals. ESR is a highly sensitive technique to study spin dynamics and magnetic interactions in a variety of compounds. In particular, the CEF effect is a higher-order effect in the Eu^{2+} ($S = 7/2$) ground state. As such, they are excellent ESR probes to study magnetic properties which purely reflect the details of RKKY magnetic interaction and FS effects in intermetallic magnetic materials.^{4,6} These studies can reveal details about the microscopic interaction J_{fs} between the $4f$ electrons and the CEs and about the Eu^{2+} - Eu^{2+} magnetic correlations.

Single-crystalline samples of EuIn_2As_2 were grown using the flux technique with starting composition $\text{Eu:As:In} = 1:2:25$. The mixture was placed in an alumina crucible and sealed in a quartz tube under vacuum. The sealed tube was heated up to $900 \text{ }^\circ\text{C}$ for 2 h and then cooled down to $400 \text{ }^\circ\text{C}$ at $2 \text{ }^\circ\text{C/h}$. The flux was then removed by centrifugation. The crystal structure and phase purity were determined by x-ray powder diffraction. Specific-heat measurements were performed in a Quantum Design physical properties measurement system (PPMS) small-mass calorimeter that employs a quasiadiabatic thermal relaxation technique. The in-plane resistivity was measured using a standard four-probe method also in the Quantum Design PPMS. The magnetization was measured using a superconducting quantum interference device magnetometer MPMS5 (Quantum Design). ESR measurements were performed in a BRUKER spectrometer equipped with a continuous He gas-flow cryostat. X-band ($\nu \sim 9 \text{ GHz}$) and Q-band ($\nu \sim 34 \text{ GHz}$) frequencies were used in the temperature region $4.2 < T < 300 \text{ K}$.

II. RESULTS AND DISCUSSION

The global physical properties of our single crystals of EuIn_2As_2 are presented in Fig. 1. Panel (a) of Fig. 1 displays the magnetic susceptibility as a function of temperature for a magnetic field $H = 1$ kOe applied parallel to the hex-plane and to the c -axis. $\chi(T)$ shows a Curie-Weiss (CW) behavior at high- T followed by an AFM transition at $T_N = 16$ K, as previously reported.⁵ From the CW magnetic susceptibility fittings for $T < T_N$ [solid lines in Fig. 1(a)] we obtained for both directions a CW temperature of $\theta_{\text{CW}} \approx 16$ K and an effective moment of $\mu_{\text{eff}} \approx 7.4 \mu_B$ for Eu^{2+} in EuIn_2As_2 , which is in agreement with the theoretical value.

The T -dependence of electrical resistivity measured in our single crystals of EuIn_2As_2 is shown in Fig. 1(b). A metallic behavior is observed in the paramagnetic regime and a clear peak appears at $T_N = 16$ K. This peak resembles the behavior observed for EuB_6 single crystals where the presence of magnetic polarons dominates the electron scattering near the ferromagnetic transition.⁷

The AFM transition can also be clearly observed in panel (c) of Fig. 1, which shows the specific heat per mole divided by temperature. The sharp main peak in C/T corresponding to the onset of AFM order can be seen at $T_N \approx 16$ K in very good agreement with the temperature where the maximum in the magnetic susceptibility occurs [see Fig. 1(a)]. The estimated magnetic entropy recovered at T_N roughly

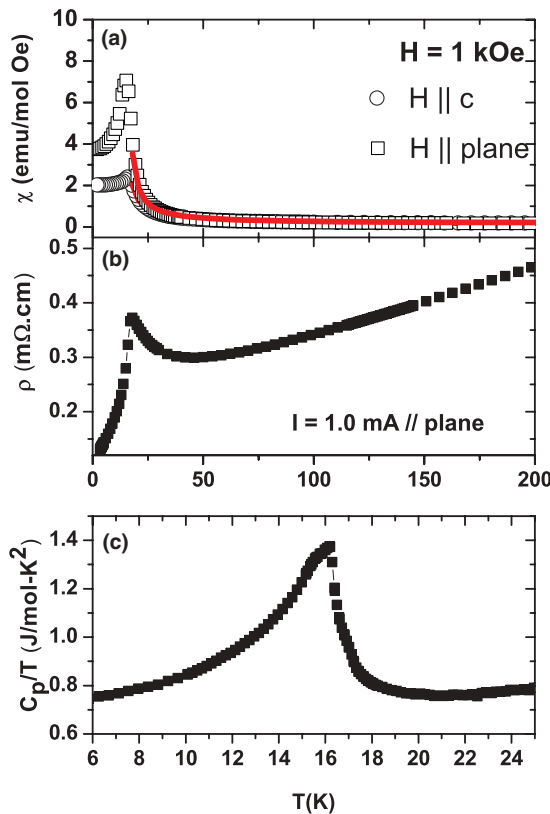


FIG. 1. (Color online) Temperature dependence of macroscopic physical properties of EuIn_2As_2 single crystals. (a) Magnetic susceptibility with applied field $H = 1$ kOe parallel to the hex-plane and to the c -axis. (b) Electrical in-plane resistivity. (c) Specific heat per mole divided by temperature.

reaches the value of $R \ln 8$ expected for the Eu^{2+} $S = 7/2$ (not shown).

Figure 2 shows the ESR spectra measured at $T = 100$ K at X - and Q -bands. In both cases we observe a single ESR resonance with a Dysonian line-shape resonance which is characteristic of localized magnetic moments in a lattice with a skin depth smaller than the size of the sample particles.⁸ From the fitting of the resonances to the appropriate admixture of absorption and dispersion, we obtain at $T = 100$ K a g -factor $g = 1.95(1)$ and a linewidth $\Delta H = 600(30)$ Oe in the X -band and $g = 1.98(1)$ and $\Delta H = 660(30)$ Oe for the Q -band for $H \parallel c$. On the other hand, for the $H \parallel \text{hex-plane}$ we obtain at $T = 100$ K a g -factor $g = 2.00(1)$ and a linewidth $\Delta H = 480(20)$ Oe in the X -band and $g = 2.01(1)$ and $\Delta H = 470(20)$ Oe for the Q -band.

Using the g -value of the Eu^{2+} in insulators as 1.993(2) we extract for both bands an apparent small g -shift which is negative ($\Delta g < 0$) for $H \parallel c$ and positive ($\Delta g > 0$) for the $H \parallel \text{hex-plane}$.⁹ This small effect may be indicative of an anisotropic $\text{Eu}^{2+} - \text{Eu}^{2+}$ magnetic coupling which seems to be consistent with the previous suggestion that there is a ferromagnetic $\text{Eu}^{2+} - \text{Eu}^{2+}$ interaction in the hex-plane and a weaker antiferromagnetic $\text{Eu}^{2+} - \text{Eu}^{2+}$ interaction between the layers.⁵ However, we can not rule out the contribution of demagnetization effects on this apparent g anisotropy.

Interestingly, the Eu^{2+} ESR ΔH also show an anisotropic behavior in Fig. 2. ΔH are clearly narrower for the $H \parallel \text{hex-plane}$ orientation for both X and Q bands. Furthermore, the Eu^{2+} ESR ΔH is nearly frequency and field independent for the $H \parallel \text{hex-plane}$ but shows a measurable broadening at the Q -band for $H \parallel c$.

The ΔH and the g -value temperature dependence for both X - and Q -bands are presented in Fig. 3. For both bands, ΔH shows a nearly constant behavior for $T > 100$ K indicating an absence of Korringa-like relaxation of Eu^{2+} spins in this temperature region. At lower temperatures, the ESR ΔH starts to broaden as a consequence of the development of short-range magnetic correlation. The X -band data show a linewidth maxima at ~ 16 K for both orientations. It is worth noting that ESR linewidth maxima do not necessarily occur at

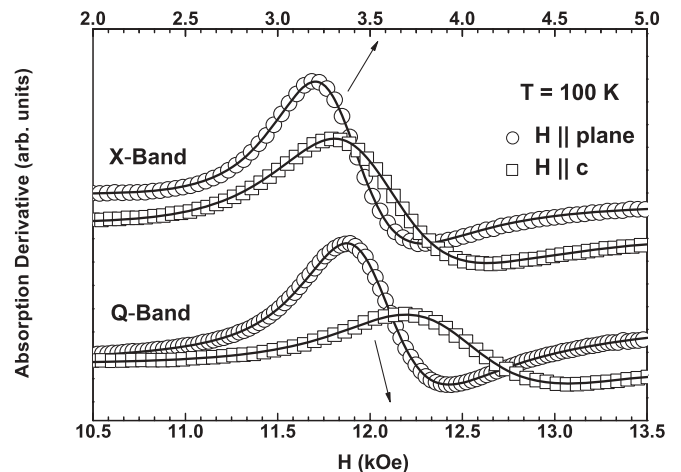


FIG. 2. X - and Q -bands Eu^{2+} ESR spectra at $T = 100$ K for H parallel to the hex-plane and to the c -axis of EuIn_2As_2 single crystals.

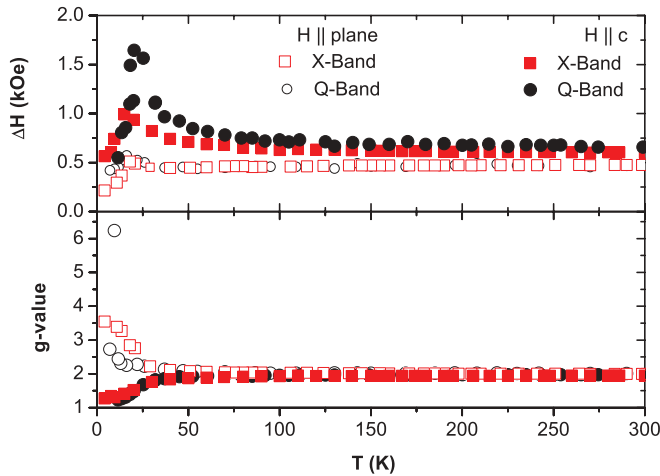


FIG. 3. (Color online) Temperature dependence of Eu^{2+} ESR ΔH and g -factor in Q - and X -bands.

T_N as they can be affected by the details of the field-dependent short-range correlations. These correlations define how the distribution of local fields decreases as the long-range ordered state develops. For fields of $\sim 1T$ (Q -band) the magnetic susceptibility data show that T_N slightly decreases for $H \parallel c$. For the $H \parallel \text{hex-plane}$ no AFM transition is observed, suggesting that the $H \parallel \text{hex-plane}$ orientation is the easy axis for a weak ferromagnetic ordering (canted antiferromagnetism). The Q -band data show a slightly higher linewidth maximum temperature for $H \parallel c$, suggesting that at higher fields stronger magnetic correlations start to affect the Eu^{2+} ESR linewidth at higher- T . At the same temperature regions, we observe a strong anisotropy in the g -value which is probably associated with the anisotropic internal field at the Eu^{2+} site. The internal field is also dependent on the applied magnetic field direction and strength. In particular we note that the Q -band g -factor for the $H \parallel \text{plane}$ increases strongly due to the presence of weak ferromagnetic ordering.

In order to understand the anisotropic field and the temperature dependence of the ESR ΔH shown in Figs. 2 and 3, different contributions to the ESR linewidth must be considered. There are two types of resonant line broadening in solids: homogeneous and inhomogeneous broadening. Homogeneous ESR linewidth is inversely proportional to the so-called *spin-spin* relaxation time, T_2 .⁹ It occurs when the magnetic resonance signal results from a transition between two spin levels which are not sharply defined but instead are somewhat intrinsically broadened. The main contributions to homogeneous broadening are (1) dipolar interaction between like spins, (2) spin-lattice interaction, (3) interaction with radiation field, (4) diffusion of excitation throughout the sample, and (5) motionally narrowing fluctuations of local fields.^{9,11}

On the other hand, an inhomogeneously broadened resonant line is one which consists of a spectral distribution of individual lines merged into an overall line or envelope. For instance, a distribution of local fields caused by unresolved fine and/or hyperfine structure, g -value anisotropy, strain distribution, and/or crystal irregularities that exceed the natural linewidth ($2/\gamma T_2$, γ is the gyromagnetic factor) will cause the spins in various parts of the sample to feel different field strengths.^{9,11}

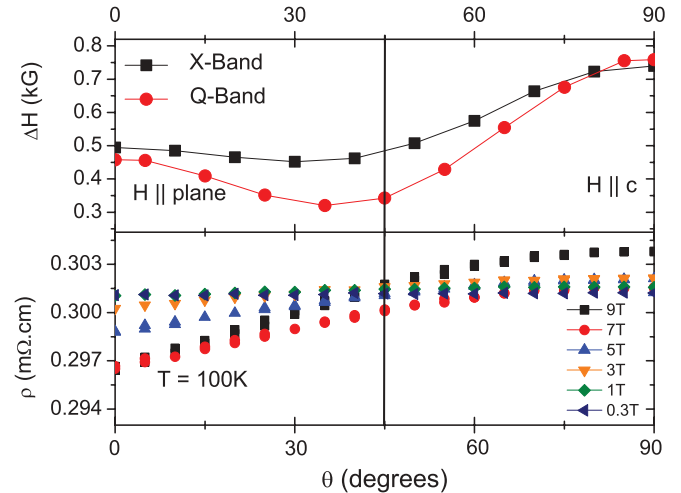


FIG. 4. (Color online) (Upper panel) Q - and X -bands Eu^{2+} ESR ΔH anisotropy at $T = 100$ K. (Lower panel) Resistivity anisotropy for several applied magnetic fields at $T = 100$ K.

In this way the resonance will be artificially broadened in an inhomogeneous manner. In the cases of inhomogeneous broadening caused by g -value anisotropy and related strain distribution and/or crystal irregularities, the ESR linewidths are expected to increase as a function of magnetic field. From the ΔH data in Fig. 2 we can conclude that the anisotropic ESR ΔH revealed a small inhomogeneous contribution when $H \parallel c$ as it presented a measurable broadening at the Q -band.

To further explore the microscopic origin of the Eu^{2+} ESR ΔH anisotropy and its small inhomogeneous contribution when $H \parallel c$ we have performed detailed angular dependent ESR and electrical resistivity experiments in the paramagnetic regime, Fig. 4. The comparison between the anisotropy in Eu^{2+} ESR ΔH with that in the electrical resistivity is important in this case because an anisotropic exchange interaction between the Eu^{2+} $4f$ electrons and the CEs would result in similar angular dependence of both physical quantities.⁷

In Fig. 4, we observe a small anisotropy in the resistivity that increases with applied magnetic field when the field is rotated from the hex-plane to the c -axis. The resistivity values are systematically larger for $H \parallel c$. On the other hand, ESR ΔH shows a much larger anisotropy but it also increases with H , being larger for the Q -band. Although the ΔH are also larger for $H \parallel c$ the angular dependence of the ΔH is obviously very distinct from that in the resistivity. This indicates that the anisotropy in these physical quantities can not have a unique common origin.

In fact the anisotropy found for Eu^{2+} ESR ΔH is reminiscent of the crystalline electrical field (CEF) anisotropy found for $S = 7/2$ ions in hexagonal systems.¹⁰ Therefore, the Eu^{2+} ESR ΔH in EuIn_2As_2 is mainly a result of an exchanged narrowed ΔH with a distribution of local fields caused by unresolved fine (CEF splitting) and perhaps hyperfine structure. As such, for $H \parallel c$, the CEF splitting of the lines is larger and generates a broader envelope line. In this direction, this inhomogeneous contribution in ΔH is large enough to overcome the exchange narrowing effect and present the broadening in the Q -band.

Therefore, the small anisotropy in the resistivity data may reflect to some extent an anisotropic magnetic scattering due to an anisotropic exchange interaction between the Eu^{2+} $4f$ electrons and the CEs. However this effect, if present in the Eu^{2+} ESR ΔH anisotropy, is overcome by the hexagonal crystal field and the Eu^{2+} - Eu^{2+} exchange narrowing effect.

In a broader scenario it is interesting to compare the results reported here for EuIn_2As_2 to the physical properties of the Fe-analog EuFe_2As_2 , which exhibits a spin-density-wave transition at $T_{\text{SDW}} = 190$ K and an antiferromagnetic transition at $T_N = 19$ K, which is slightly higher than $T_N = 16$ K in EuIn_2As_2 , in agreement with the smaller separation between Eu first neighbor ions ($a = 3.907$ Å) in comparison with EuIn_2As_2 where $a = 4.2067$ Å. ESR measurements on EuFe_2As_2 show, for $T > T_{\text{SDW}}$, a Korringa-like increase of the ESR ΔH of $b = 6.5$ – 8.0 Oe/K.^{12–15} Recent ESR studies for several Eu^{2+} concentrations in $\text{Ba}_{1-x}\text{Eu}_x\text{Fe}_2\text{As}_2$ have revealed that this Korringa rate systematically decreases with decreasing x and it is absent in the dilute regime.¹⁶ This suppression of the Korringa rate towards the Ba-rich compounds was claimed to be a result of the reduction of the q -dependent exchange interaction between the Eu^{2+} f electrons and the CEs, which is likely associated with an increasing of localization of Fe d electrons with decreasing x .¹⁶

The absence of Korringa behavior reported here for concentrated EuIn_2As_2 for $T > 100$ K provides a irrefutable confirmation that the behavior described above for the FeAs-based compounds is indeed due to the relaxation of Eu^{2+} via Fe $3d$ electrons.

III. CONCLUSION

We report here ESR experiments on single-crystalline samples of EuIn_2As_2 , which crystallizes with a hexagonal structure, space group $P6(3)/mmc$, and presents AFM ordering below $T_N = 16$ K. In the paramagnetic state, a single Eu^{2+} Dysonian ESR line with nearly temperature-independent g -factor and linewidth is observed, indicating the absence of Korringa-like relaxation of the Eu^{2+} ions. Approaching the antiferromagnetic transition, we observe an anisotropic g -shift and a linewidth broadening which has a maximum in the transition temperature, suggesting that the short-range AFM correlation dominates the spin dynamics of the Eu^{2+} spin in the temperature range. The anisotropy of the ESR linewidth at high- T indicated the presence of exchanged narrowed Eu^{2+} fine structure suggesting the presence of CEF effects. The absence of Korringa behavior reported here for concentrated EuIn_2As_2 for $T > 100$ K is an important result to confirm the dominant role of the Fe $3d$ electronic states in the Eu^{2+} spin dynamics and in the formation of the SDW found in its FeAs-based analogs.

ACKNOWLEDGMENTS

This work was supported by Fundação de Amparo à Pesquisa do Estado de São Paulo (Grants No. 2006/60440-0, No. 2009/09247-3, No. 2010/11949-3, No. 2011/01564-0, and No. 2011/23650-5), National Council for Scientific and Technological Development, and Financiadora de Estudos e Projetos, Brazil.

¹A. Szytula *et al.*, *Materials Science – Poland* **25**, 3 (2006).

²H. V. Löhneysen *et al.*, *Rev. Mod. Phys.* **79**, 1015 (2007).

³G. R. Stewart, *Rev. Mod. Phys.* **83**, 1589 (2011).

⁴P. G. Pagliuso, J. D. Thompson, M. F. Hundley, J. L. Sarrao, and Z. Fisk, *Phys. Rev. B* **63**, 054426 (2001).

⁵A. M. Goforth *et al.*, *Inorg. Chem.* **47**, 11048 (2008).

⁶E. Granado, P. G. Pagliuso, C. Giles, R. Lora-Serrano, F. Yokaichiya, and J. L. Sarrao, *Phys. Rev. B* **69**, 144411 (2004).

⁷R. R. Urbano, P. G. Pagliuso, C. Rettori, S. B. Oseroff, J. L. Sarrao, P. Schlottmann, and Z. Fisk, *Phys. Rev. B* **70**, 140401(R) (2004).

⁸F. J. Dyson, *Phys. Rev.* **98**, 349 (1955).

⁹A. Abragam and B. Bleaney, *Electron Paramagnetic Resonance of Transition Ions* (Clarendon, Oxford, 1970).

¹⁰P. M. Zimmerman *et al.*, *Phys. Rev. B* **6**, 2783 (1972); J. Nagel and K. Baberschke, in *Crystal Field Effects in Metals*, edited by A. Furrer (Plenum, New York, 1977), p. 66; G. Lacueva, P. M. Levy, and A. Fert, *Phys. Rev. B* **31**, 6245 (1985).

¹¹C. P. Poole and H. A. Farach, *Relaxation in Magnetic Resonance* (Academic, New York, 1971).

¹²E. Dengler, J. Deisenhofer, H. A. Krug von Nidda, S. Khim, J. S. Kim, K. H. Kim, F. Casper, C. Felser, and A. Loidl, *Phys. Rev. B* **81**, 024406 (2010).

¹³N. Pascher, J. Deisenhofer, H. A. Krug von Nidda, M. Hemmida, H. S. Jeevan, P. Gegenwart, and A. Loidl, *Phys. Rev. B* **82**, 054525 (2010).

¹⁴J. J. Ying *et al.*, *Phys. Rev. B* **81**, 052503 (2010).

¹⁵F. A. Garcia *et al.*, *New J. Phys.* **14**, 063005 (2012).

¹⁶P. F. S. Rosa *et al.* (unpublished).